



HAL
open science

Properties of $\text{In}_x\text{Ga}_{1-x}\text{N}$ films in terahertz range

A. Gauthier-Brun, J.H. Teng, El Hadj Dogheche, W. Liu, A. Gokarna, M. Tonouchi, S.J. Chua, Didier Decoster

► **To cite this version:**

A. Gauthier-Brun, J.H. Teng, El Hadj Dogheche, W. Liu, A. Gokarna, et al.. Properties of $\text{In}_x\text{Ga}_{1-x}\text{N}$ films in terahertz range. Applied Physics Letters, 2012, 100, pp.071913-1-5. 10.1063/1.3684836 . hal-00787430

HAL Id: hal-00787430

<https://hal.science/hal-00787430>

Submitted on 27 May 2022

HAL is a multi-disciplinary open access archive for the deposit and dissemination of scientific research documents, whether they are published or not. The documents may come from teaching and research institutions in France or abroad, or from public or private research centers.

L'archive ouverte pluridisciplinaire **HAL**, est destinée au dépôt et à la diffusion de documents scientifiques de niveau recherche, publiés ou non, émanant des établissements d'enseignement et de recherche français ou étrangers, des laboratoires publics ou privés.

Properties of $\text{In}_x\text{Ga}_{1-x}\text{N}$ films in terahertz range

Cite as: Appl. Phys. Lett. **100**, 071913 (2012); <https://doi.org/10.1063/1.3684836>

Submitted: 31 August 2011 • Accepted: 17 January 2012 • Published Online: 17 February 2012

A. Gauthier-Brun, J. H. Teng, E. Dogheche, et al.



View Online



Export Citation

ARTICLES YOU MAY BE INTERESTED IN

[Terahertz carrier dynamics and dielectric properties of GaN epilayers with different carrier concentrations](#)

Journal of Applied Physics **106**, 063104 (2009); <https://doi.org/10.1063/1.3212966>

[Terahertz studies of carrier dynamics and dielectric response of n-type, freestanding epitaxial GaN](#)

Applied Physics Letters **82**, 2841 (2003); <https://doi.org/10.1063/1.1569988>

[Tutorial: An introduction to terahertz time domain spectroscopy \(THz-TDS\)](#)

Journal of Applied Physics **124**, 231101 (2018); <https://doi.org/10.1063/1.5047659>

Lock-in Amplifiers
up to 600 MHz



Zurich
Instruments



Properties of $\text{In}_x\text{Ga}_{1-x}\text{N}$ films in terahertz range

A. Gauthier-Brun,^{1,2,a)} J. H. Teng,¹ E. Dogheche,² W. Liu,¹ A. Gokarna,² M. Tonouchi,³ S. J. Chua,¹ and D. Decoster²

¹*Institute of Materials Research and Engineering (IMRE), Agency for Science, Technology and Research (A*STAR), 3 Research link, Singapore 117602, Singapore*

²*Institute of Electronics, Microelectronics and Nanotechnology, UMR-CNRS 8520, Avenue Poincaré, 59652 Villeneuve d'Ascq Cedex, France*

³*Institute of Laser Engineering, Osaka University, 2-6 Yamada-Oka, Suita-City, Osaka 565-0871, Japan*

(Received 31 August 2011; accepted 17 January 2012; published online 17 February 2012)

In this letter, we report the characterization of the refractive indices and complex conductivities of a set of GaN films with different carrier concentrations, InN film, and $\text{In}_x\text{Ga}_{1-x}\text{N}$ films with indium content varying from $x = 0.07$ to $x = 0.14$ grown by metalorganic chemical vapor deposition for frequencies ranging from 0.3 to 3 THz using terahertz time-domain spectroscopy (THz-TDS). The refractive indices of $\text{In}_x\text{Ga}_{1-x}\text{N}$ films at THz range are reported. The carrier density and mobility determined using THz-TDS method show good agreement with four-probe Hall measurements.

© 2012 American Institute of Physics. [doi:10.1063/1.3684836]

The $\text{In}_x\text{Ga}_{1-x}\text{N}$ compound is a promising ternary alloy system which receives a lot of attentions thanks to its tunable band gap that varies from the near infrared region of ~ 0.7 eV (InN) to the near ultraviolet region of ~ 3.4 eV (GaN).¹ InGaN/GaN materials have been widely used in various applications like high efficiency solar cells,² high-brightness blue to green light emitting diodes,³ or laser diodes,⁴ as well as non-phosphor based direct white light generation.⁵ The unique properties of this material like the high break down field, large electron saturation velocity, and chemical stability at high temperature also make them a promising candidate for high power electronics for micro- and milli-metre waves, especially terahertz (THz) waves in which highly efficient emitters and detectors are still bottlenecks.⁶ Recently, there have been reports on using InN and InGaN/GaN quantum wells for THz generation.⁷⁻⁹ To design an efficient InGaN/GaN based THz device, it is a prerequisite to know the optical properties of $\text{In}_x\text{Ga}_{1-x}\text{N}$ films at the frequencies of interest. Terahertz responses of GaN¹⁰⁻¹³ and more recently InN¹⁴ epilayers have been reported using terahertz time-domain spectroscopy (THz-TDS), and conductivities have been determined using a simple Drude model. Optical properties of high In content $\text{In}_x\text{Ga}_{1-x}\text{N}$ materials in visible range have also been studied,¹⁵⁻¹⁷ but the properties of this compound over the terahertz range have yet to be reported.

In this letter, we report the characterization of the refractive indices of $\text{In}_x\text{Ga}_{1-x}\text{N}$ films with In concentration of $x = 0$, $x = 0.07$, $x = 0.10$, $x = 0.14$, and $x = 1$ for frequencies ranging from 0.3 to 3 THz using THz-TDS. GaN samples with different doping levels are used to study the effect of the carrier concentration on the optical and electrical responses in the THz range and to benchmark with the literature reports. The $\text{In}_x\text{Ga}_{1-x}\text{N}$ samples are grown by metalorganic chemical vapor deposition (MOCVD) on GaN template on (0001) sapphire substrate. The precursors utilized are trimethylgallium, trimethylindium, and ammonia

for gallium, indium, and nitrogen, respectively. First, a thin (~ 35 nm) GaN seed layer is grown on a sapphire substrate at low temperature (~ 530 °C) followed by high temperature (~ 1050 °C) growth of an undoped GaN layer with a thickness of about $2 \mu\text{m}$. In the case of $\text{In}_x\text{Ga}_{1-x}\text{N}$ samples, a 200 nm–300 nm-thick $\text{In}_x\text{Ga}_{1-x}\text{N}$ layer as measured by cross-sectional scanning electron microscopy (SEM) with In contents of $x = 0.07$, $x = 0.10$, and $x = 0.14$ is then grown at different growth temperatures and determined using x-ray diffraction (XRD) and secondary ion mass spectroscopy (SIMS).¹⁷ For the InN sample, a 50 nm-thick $\text{In}_{0.3}\text{Ga}_{0.7}\text{N}$ layer is grown as a transition layer, followed by a 300 nm-thick InN layer. For the GaN samples, one undoped GaN (u-GaN) and two n-type Si-doped GaN (n-GaN) with respective carrier concentrations of $2.5 \times 10^{17} \text{ cm}^{-3}$, $1.8 \times 10^{18} \text{ cm}^{-3}$, and $3.3 \times 10^{18} \text{ cm}^{-3}$ and thicknesses of $2 \mu\text{m}$, $3.8 \mu\text{m}$, and $2.1 \mu\text{m}$ are grown. Mobility and carrier density are characterized by four-probe Hall measurements and compared with the values obtained from the THz-TDS analysis. The THz-TDS data are obtained using a TeraView Spectra 3000 system, in which the THz wave is generated by focusing a mode-locked Ti:sapphire laser beam with a wavelength of 800 nm and pulse width of ~ 100 fs onto a low temperature-grown GaAs photoconductive antenna. The generated THz wave is collimated and focused on the samples by off-axis parabolic gold-coated mirrors. The set-up is placed in a chamber purged with dry nitrogen to minimize the water vapor absorption.

The THz-TDS method determines the optical properties of a thin layer by comparing it with another layer of known index. In the sample characterization, we remove the part of the layer of interest by inductively coupled plasma (ICP) etching using Cl_2 and BCl_3 gases to compare and analyze the THz-TDS signals from the as-grown layer structure and the top layer-removed sample. The THz-TDS measurement is done in two steps: we first compare the THz-TDS signals through the empty chamber and the effective substrate, e.g., sapphire (0001) in the case of GaN samples, to determine the index of the substrate. Then, we compare the signals going

^{a)}Electronic mail: a.gauthier-brun@ed.univ-lille1.fr.

through this effective substrate and through the as-grown sample. Through comparing the THz transmission spectra, we can obtain the properties of the top layer.

Figure 1 shows the temporal signal of the THz pulses and their Fourier transform, respectively, for the u-GaN sample. We do not take into account multiple reflections in the sample, so only the data from the initial peak are represented and used for the analysis. The transmission coefficient of a pulse propagating through a sample of known thickness and index is given by

$$H(\omega) = \frac{E_{film}(\omega)}{E_{ref}(\omega)} = \frac{2n(n_s + 1)e^{i(n-1)\omega d/c}}{(n+1)(n+n_s) + (1-n)(n-n_s)e^{i2n\omega d/c}}, \quad (1)$$

where $n(\omega)$ and $n_s(\omega)$ are the refractive indices of the layer of interest and the effective substrate, respectively, and d is the thickness of the layer that was etched away. By fitting numerically Eq. (1) to the measured transmission function, we can extract the value of $n(\omega)$. The dielectric function $\varepsilon(\omega)$ and the complex conductivity $\sigma(\omega)$ are determined as

$$\varepsilon(\omega) = n(\omega)^2 = \varepsilon_{dc} + i \frac{\sigma(\omega)}{\omega \varepsilon_0} \quad (2)$$

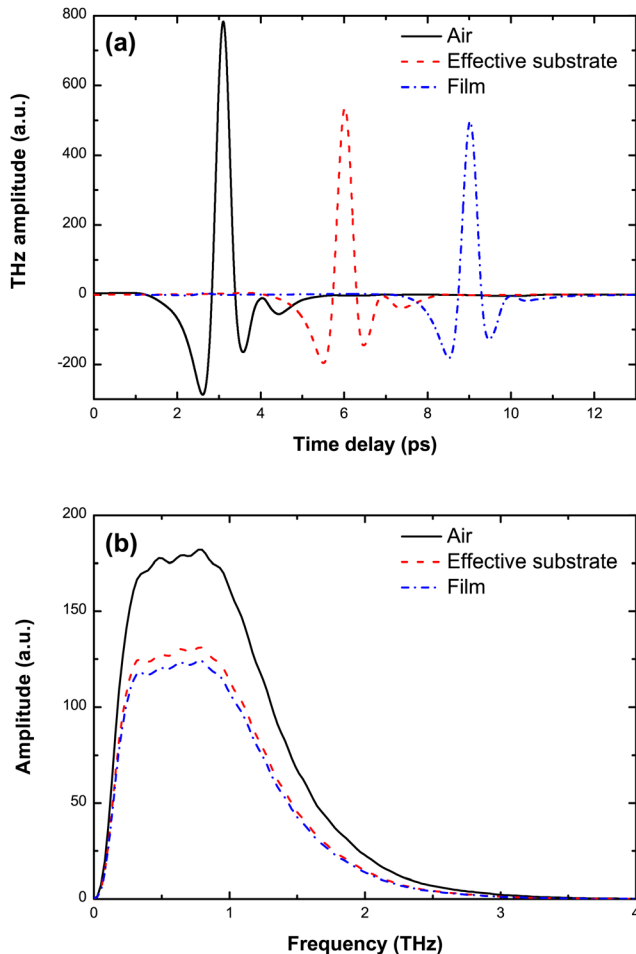


FIG. 1. (Color online) Terahertz time domain spectra (a) and their Fourier transform spectra (b) transmitted through the nitrogen-filled chamber (air), the etched part of a GaN sample (effective substrate), and the entire sample (film). For clarity, the later was shifted of +3 ps.

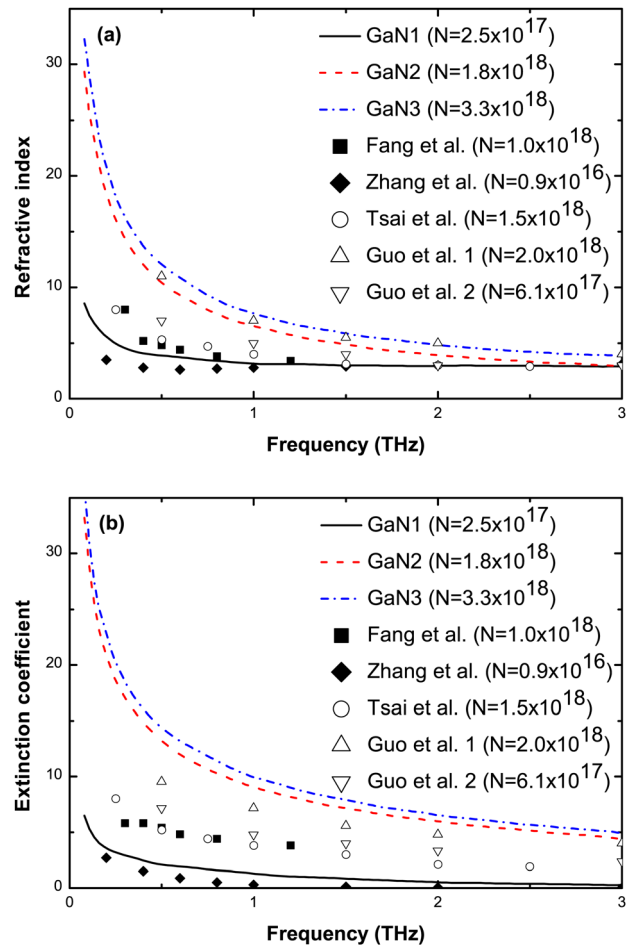


FIG. 2. (Color online) Real (a) and imaginary (b) parts of the refractive index for three GaN samples (lines) with different carrier concentrations (values between brackets) and comparison with values provided in other works by Fang *et al.* (see Ref. 13), Zhang *et al.* (see Ref. 10), Tsai *et al.* (see Ref. 11), and Guo *et al.* (see Ref. 12) (symbols).

with ε_{dc} being the dielectric constant. $\varepsilon_{dc} = 9.4$,¹⁸ and 13.1¹⁹ for GaN and InN, respectively. There are no calculated or measured values for $\text{In}_x\text{Ga}_{1-x}\text{N}$, so we assume the dielectric constant to be similar to GaN given the low value of x for our samples.

In semiconductors, the free carrier contribution to the properties of the material at long wavelength below the bandgap is determined by the intraband transitions of the partially filled band. Omitting the restoring force of the free carriers, this leads to the simple Drude model for which the complex conductivity $\sigma(\omega)$ is related to the carrier concentration N and the mobility μ ,

$$\sigma(\omega) = \frac{\varepsilon_0 \omega_p^2 \tau_0}{1 - i\omega \tau_0}, \quad (3)$$

where ω_p is the plasma frequency $\omega_p^2 = \frac{Ne^2}{\varepsilon_0 m^*}$ and the relaxation time $\tau_0 = \frac{\mu m^*}{e}$, where m^* is the effective electron mass. The value of m^* is taken as $0.22m_0$ ²⁰ and $0.14m_0$ ²¹ for GaN and InN, respectively, with m_0 the mass of the free electron. Due to the lack of values for m^* for $\text{In}_x\text{Ga}_{1-x}\text{N}$ for our compositions, we use the GaN effective electron mass for $\text{In}_x\text{Ga}_{1-x}\text{N}$. The values of N and μ are extracted by fitting the conductivity from the THz-TDS analysis and are finally

compared to the carrier concentration and mobility from the four-probe Hall measurements.

Figure 2 presents the real and imaginary parts of the refractive indices for the three GaN samples with different carrier concentrations extracted from the THz-TDS numerical fitting and those of GaN samples previously reported.¹⁰⁻¹³ At 1 THz, the refractive index is determined to be 3.14 for u-GaN ($N = 2.7 \times 10^{17} \text{ cm}^{-3}$), 6.48 and 7.62 for n-GaN at $N = 1.8 \times 10^{18} \text{ cm}^{-3}$ and $N = 3.3 \times 10^{18} \text{ cm}^{-3}$, respectively. The index measured by Zhang *et al.*¹⁰ for a sample with a smaller carrier concentration ($N = 0.9 \times 10^{16} \text{ cm}^{-3}$) is lower at ~ 2.8 , while Fang *et al.*,¹³ Tsai *et al.*,¹¹ and Guo *et al.*¹² provide intermediate values ranging from ~ 3.6 to ~ 7 for carrier concentrations between $N = 6.1 \times 10^{17} \text{ cm}^{-3}$ and $N = 2.0 \times 10^{18} \text{ cm}^{-3}$. At frequency higher than 2 THz, the difference of refractive indices for different doping concentrations in GaN sample becomes smaller, while at frequency lower than 1 THz, the refractive index of the highly doped

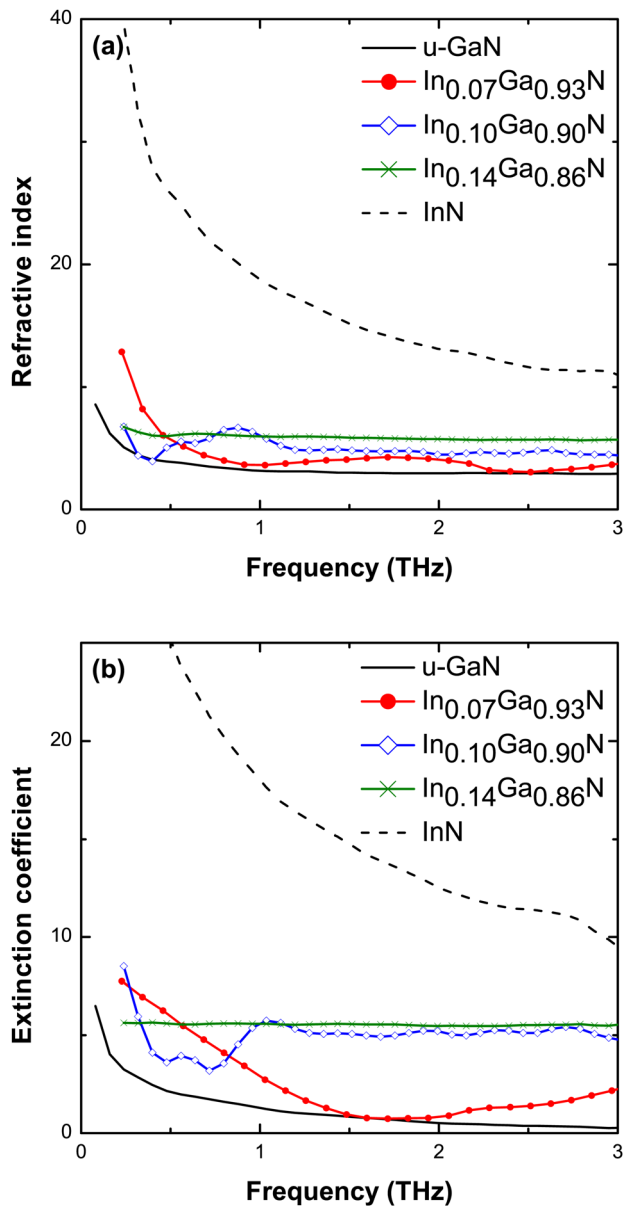


FIG. 3. (Color online) Real (a) and imaginary (b) parts of the refractive indices of a set of $\text{In}_x\text{Ga}_{1-x}\text{N}$ samples with different indium contents. $x = 0$ (GaN), $x = 0.07$, $x = 0.11$, $x = 0.14$, and $x = 1$ (InN).

GaN sample increases quickly due to the stronger plasma effect. The optical index depends on both carrier concentration and mobility, but the carrier concentration varies by two orders of magnitude ($\sim 10^{16} \text{ cm}^{-3}$ to $\sim 10^{18} \text{ cm}^{-3}$) while the mobility varies by just one order ($\sim 10^2 \text{ cm}^2 \text{ s}^{-1} \text{ V}^{-1}$ to $\sim 10^3 \text{ cm}^2 \text{ s}^{-1} \text{ V}^{-1}$) as determined by Hall measurements for our samples. Since the conductivity varies more with the large variations in the carrier concentration, so do the dielectric function and the optical index.

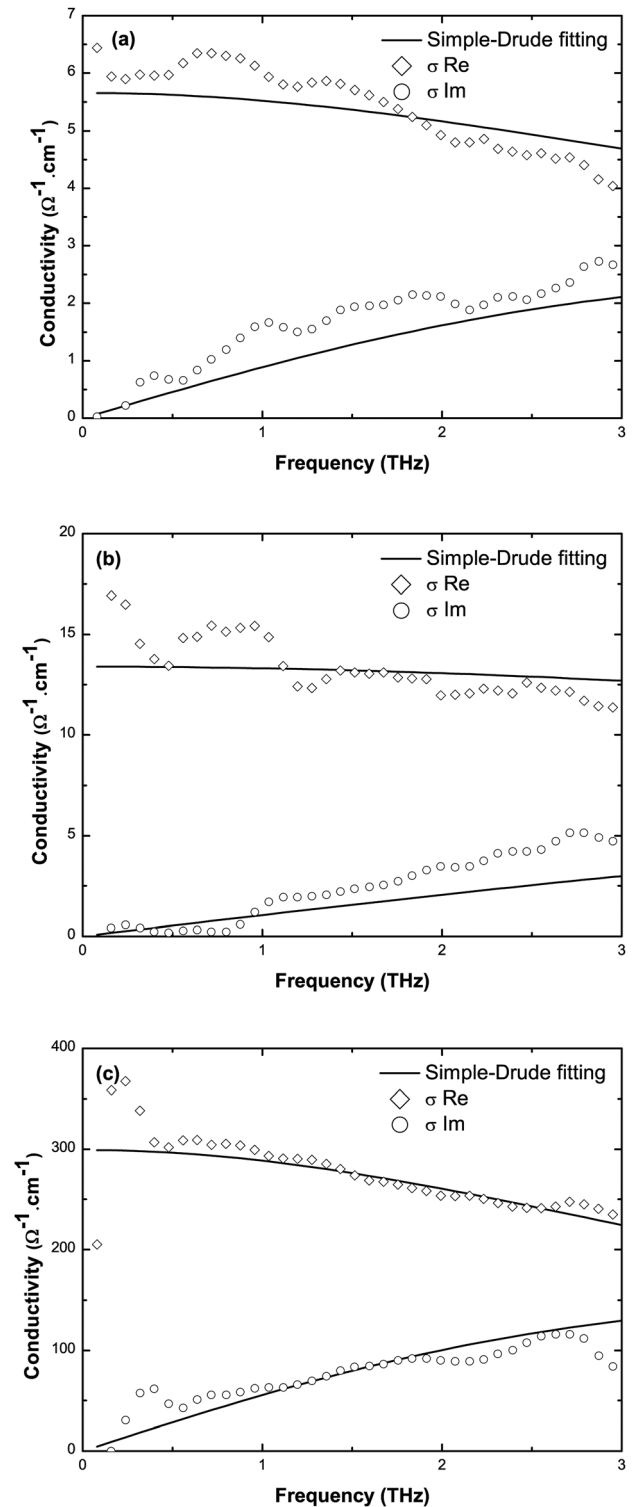


FIG. 4. Real (lozenges) and imaginary (circles) parts of the conductivities of GaN (a), $\text{In}_{0.07}\text{Ga}_{0.93}\text{N}$ (b), and InN (c) samples. The best fit using a Simple-Drude model is displayed in plain lines.

TABLE I. Free carrier density N and mobility μ obtained by four-probe contact measurements and THz-TDS analysis for GaN, $\text{In}_x\text{Ga}_{1-x}\text{N}$, and InN.

Sample	N TDS (cm^{-3})	N Hall (cm^{-3})	μ TDS ($\text{cm}^2 \text{s}^{-1} \text{V}^{-1}$)	μ Hall ($\text{cm}^2 \text{s}^{-1} \text{V}^{-1}$)
4.0 μm u-GaN	1.10×10^{17}	2.50×10^{17}	245	124
5.8 μm n-GaN	1.10×10^{18}	1.80×10^{18}	436	337
4.1 μm n-GaN	1.90×10^{18}	3.30×10^{18}	300	260
200 nm $\text{In}_{0.07}\text{Ga}_{0.93}\text{N}$	7.20×10^{17}	5.10×10^{17}	91	94.2
200 nm $\text{In}_{0.10}\text{Ga}_{0.90}\text{N}$	7.60×10^{17}	6.40×10^{17}	83	92.5
300 nm $\text{In}_{0.14}\text{Ga}_{0.86}\text{N}$	1.00×10^{18}	6.50×10^{17}	80	92.4
300 nm n-InN	2.60×10^{18}	4.40×10^{18}	718	580

The refractive indices and extinction coefficients for u-GaN (black solid line), $\text{In}_x\text{Ga}_{1-x}\text{N}$ with $x = 0.07$ (red circle), $x = 0.10$ (blue lozenge) and $x = 0.14$ (green cross) and InN (black dotted line) are presented in Figure 3. The indices of $\text{In}_x\text{Ga}_{1-x}\text{N}$ are between the ones of GaN and InN and are ordered by indium atomic fraction. At 1 THz, the refractive index of GaN, $\text{In}_{0.07}\text{Ga}_{0.93}\text{N}$, $\text{In}_{0.10}\text{Ga}_{0.90}\text{N}$, $\text{In}_{0.14}\text{Ga}_{0.86}\text{N}$, and InN are 3.14, 3.61, 5.93, 5.98, and 14.63, respectively. The extinction coefficients are 1.27, 2.73, 5.58, 5.71, and 17.92, respectively. The values for $\text{In}_{0.10}\text{Ga}_{0.90}\text{N}$ and $\text{In}_{0.14}\text{Ga}_{0.86}\text{N}$ are very close to each other and do not exhibit the same gap as GaN and $\text{In}_{0.07}\text{Ga}_{0.93}\text{N}$ or $\text{In}_{0.07}\text{Ga}_{0.93}\text{N}$ and $\text{In}_{0.10}\text{Ga}_{0.90}\text{N}$. This was also observed in the optical refractive index results of the same samples in the visible range, where the refractive indices at 633 nm were 2.39, 2.40, 2.42, and 2.43 for GaN, $\text{In}_{0.07}\text{Ga}_{0.93}\text{N}$, $\text{In}_{0.10}\text{Ga}_{0.90}\text{N}$, and $\text{In}_{0.14}\text{Ga}_{0.86}\text{N}$, respectively. This is believed to be due to the alloy scattering, inhomogeneity and a growing number of defects with x , as showed by the higher V-pit density in the TEM images.¹⁷ The higher indium concentration increases the internal strain, modifying the band gap structure and resulting in a lower refractive index value.²² For InN, values are found to be around 25% smaller than the one reported previously.¹⁹ On top of the threading dislocation phenomenon, it has been observed in the SIMS analysis that gallium has diffused through the InN layer and that the indium fraction is actually varying between 0.8 and 1.

Results of the numerical iteration on the conductivity using the simple Drude model are presented in Figure 4 for non-intentionally doped GaN, $\text{In}_{0.07}\text{Ga}_{0.93}\text{N}$, and InN. The values for conductivity are of different orders of magnitude up to $6 \Omega^{-1} \text{cm}^{-1}$ for GaN, $15 \Omega^{-1} \text{cm}^{-1}$ for $\text{In}_{0.07}\text{Ga}_{0.93}\text{N}$, and $300 \Omega^{-1} \text{cm}^{-1}$ for InN.

Finally, the values of carrier concentration and mobility from THz-TDS analysis and four-probe Hall measurements are compared to check the validity of our analysis, as shown in Table I. A relatively good match is observed and the best fitted carrier concentrations and mobilities are in good agreement with the values provided by Hall measurement.

Two different behaviors are observed. For GaN and InN samples, the carrier concentration from THz-TDS is lower than the one from Hall measurements while mobility is higher in the case of THz-TDS. On the other hand, the results from $\text{In}_x\text{Ga}_{1-x}\text{N}$ seem to be a closer match but display a higher carrier concentration and a lower mobility for THz-TDS. The different natures of the measurement (in-plane for the Hall measurements, normal to the layers for THz-TDS) explain this difference, along with the varying growth quality. As shown for the conductivity of $\text{In}_{0.07}\text{Ga}_{0.93}\text{N}$, the cor-

relation between the Drude model and the measured data at any given frequency can be relative, but when integrated on the whole range, the final results are very close to the Hall measurements.

In summary, optical characterization has been conducted on GaN, InN, and $\text{In}_x\text{Ga}_{1-x}\text{N}$ in the THz frequency range through THz-TDS. The carrier concentration and mobility determined from the THz-TDS are in good agreement with those from Hall measurement. Results on GaN with different carrier concentrations and on InN are consistent with previous report and demonstrate strong relationship between carrier concentration and optical index; the refractive index and conductivity of $\text{In}_x\text{Ga}_{1-x}\text{N}$ films with In fractions of 0.07–0.14 are measured from the THz-TDS method and shown to increase with the indium concentration. These results are important for $\text{In}_x\text{Ga}_{1-x}\text{N}$ -based THz device applications.

This work was supported by funding from the CNRS and Nord Pas de Calais region in France, funding from A*STAR in Singapore with Grant No. 082 1410038, as well as a grant awarded by the Embassy of France in Singapore through its Merlion program. Thanks to Mr. Norman Ang Soo Seng for ICP etching, as well as Dr. Guo Hong Chen and Ms. Liu Hong Wei for conducting THz-TDS measurements.

¹S. Nakamura and G. Fasol, *The Blue Laser Diode* (Springer, Berlin, 1997), pp. 201–260.

²J. Wu, W. Walukiewicz, K. M. Yu, W. Shan, J. W. Ager III, E. E. Haller, H. Lu, W. J. Schaff, W. K. Metzger, and S. Kurtz, *J. Appl. Phys.* **94**, 6477 (2003).

³T. Miyoshi, S. Masui, T. Okada, T. Yanamoto, T. Kozaki, S. Nagahama, and T. Mukai, *Appl. Phys. Express* **2**, 062201 (2009).

⁴S. Nakamura, M. Senoh, N. Iwasa, S. Nagahama, T. Yamada, and T. Mukai, *Jpn. J. Appl. Phys., Part 2* **34**, L1332 (1995).

⁵C. Soh, W. Liu, J. Teng, S. Chow, S. Ang, and S. Chua, *Appl. Phys. Lett.* **92**, 261909 (2008).

⁶M. Tonouchi, *Nature Photon.* **1**, 97 (2007).

⁷T. V. Shubina, A. V. Andrianov, A. O. Zakhar'in, V. N. Jmerik, I. P. Soshnikov, T. A. Komissarova, A. A. Usikova, P. S. Kop'ev, S. V. Ivanov, V. A. Shalygin *et al.*, *Appl. Phys. Lett.* **96**, 183106 (2010).

⁸R. Ascázubi, I. Wilke, K. Denniston, H. Lu, and W. J. Schaff, *Appl. Phys. Lett.* **84**, 4810 (2004).

⁹H. Ahn, Y. P. Ku, C. H. Chuang, C. L. Pan, H. W. Lin, Y. L. Hong, and S. Gwo, *Appl. Phys. Lett.* **92**, 102103 (2008).

¹⁰W. Zhang, A. K. Azad, and D. Grischkowsky, *Appl. Phys. Lett.* **82**, 2841 (2003).

¹¹T. R. Tsai, S. J. Chen, C. F. Chang, S. H. Hsu, T. Y. Lin, and C. C. Chi, *Opt. Express* **14**, 4898 (2006).

¹²H. C. Guo, X. H. Zhang, W. Liu, A. M. Yong, and S. H. Tang, *J. Appl. Phys.* **106**, 063104 (2009).

¹³H. N. Fang, R. Zhang, B. Liu, H. Lu, J. P. Ding, Z. L. Xie, X. Q. Xiu, Y. D. Zheng, M. W. Xiao, C. H. Zhang *et al.*, *Chin. Phys. Lett.* **27**, 017802 (2010).

- ¹⁴H. Ahn, C. L. Pan, and S. Gwo, Proc. SPIE **7216**, 72160T (2009).
- ¹⁵M. Anani, H. Abid, Z. Chama, C. Mathieu, A. Sayede, and B. Khelifa, *Microelectron. J.* **38**, 262 (2007).
- ¹⁶N. A. Sanford, A. Munkholm, M. Krames, A. Shapiro, I. Levin, A. Davydov, S. Sayan, L. Wielunski, and T. Madey, *Phys. Status Solidi C* **2**, 2783 (2005).
- ¹⁷A. Gokarna, A. Gauthier-Brun, W. Liu, Y. Androussi, E. Dumont, E. Dogheche, J. H. Teng, S. J. Chua, and D. Decoster, *Appl. Phys. Lett.* **96**, 191909 (2010).
- ¹⁸A. S. Barker, Jr. and M. Ilegems, *Phys. Rev. B* **7**, 743 (1973).
- ¹⁹V. Yu. Davydov, V. V. Emtsev, I. N. Goncharuk, A. N. Smirnov, V. D. Petrikov, V. V. Mamutin, V. A. Vekshin, S. V. Ivanov, M. B. Smirnov, and T. Inushima, *Appl. Phys. Lett.* **75**, 3297 (1999).
- ²⁰W. J. Moore and J. A. Freitas, Jr., *Phys. Rev. B* **56**, 12073 (1997).
- ²¹A. Kasic and M. Schubert, *Phys. Rev. B* **65**, 115206 (2002).
- ²²F. Natali, F. Semond, J. Massies, D. Byrne, S. Lügt, O. Tottereau, P. Venéguès, E. Dogheche, and E. Dumont, *Appl. Phys. Lett.* **82**, 1386 (2003).